

# MICROANATOMY OF THE PRIMATE MOUSE LEMUR BRAIN AT 7T AFTER PASSIVE STAINING

A. Bertrand<sup>1,2</sup>, A. Petiet<sup>1,3</sup>, S. Mériaux<sup>2</sup>, C. J. Wiggins<sup>2</sup>, A. Kraska<sup>1,2</sup>, O. Dorieux<sup>1,2</sup>, F. Aujard<sup>4</sup>, and M. Dhenain<sup>1,2</sup>

<sup>1</sup>CNRS URA2210, MIRCen, Orsay, France, <sup>2</sup>Neurospin, I2BM, CEA, Gif-sur-Yvette, France, <sup>3</sup>Sanofi-Aventis R&D, Vitry-sur-Seine, France, <sup>4</sup>UMR CNRS/MNHN 7179, Mecadev, Brunoy, France

**INTRODUCTION :** Alzheimer's disease (AD) researchers have recently shown an increasing interest in the primate *Microcebus murinus*, the so-called mouse lemur, as a model of this disease (1). Unlike transgenic mice, the present reference models, mouse lemurs may, with age, spontaneously develop the two hallmarks of AD: Aβ deposits and tauopathy. Adult animals weigh approximately 100 g and have a brain that measures approximately 23 mm (from the tip of the olfactory bulbs to the caudal end of the medulla), with a maximum width of 18 mm. These characteristics, added to their phylogenetic proximity with humans, make them promising model for future research on AD. A stereotaxic atlas of the mouse lemur brain was created 10 years ago, based on 2D histological data (2). Given that micro-MRI has become a major tool in preclinical research on AD, accurate MR data on the mouse lemur brain are required before using this animal in preclinical studies. We performed a micro-MRI ex vivo study on 6 mouse lemur formalin-fixed brains using passive staining, a technique that allows for an increased signal in fixed brains through the passive diffusion of gadolinium (3).

**METHODS :** 6 mouse lemur formalin-fixed brains were used for this study. For passive staining, brains were soaked in a solution of PBS with Dotarem® (Guerbet, France) at a concentration of 2.5 mmol.L<sup>-1</sup>, for at least 24 hours. For the MRI acquisitions, brains were removed from the solution and placed in a container filled with Fluorinert® (3M, US). MR images were acquired on a 7T wholebody MRI system (Siemens, Syngo MR VB15) with maximum gradient strength of 80 mT/m and a slew rate of 333 mT/m.s. A 3D gradient-echo-based sequence was used (FLASH, TR/TE = 200/20 ms, scan time = 5-6 h depending on the brain size, resolution = 31 µm x 31 µm x 120 µm). The acquisition covered both hemispheres, plus the olfactory bulbs that were preserved in 2 brains; cerebellum and pons were not studied. One of the 6 brains was scanned twice, before and after passive staining, and was used for quantitative analysis: regions of interest (ROI) were traced in 6 white matter tracts of various thickness (corpus callosum CC, internal capsule IC, optic chiasm Opt Ch, anterior commissura AC, mamillo-thalamic tract MTT, and fornix Fx), in 6 areas of grey matter adjacent to each tract, and outside the brain, to determine the contrast-to-noise ratios (CNR) between grey and white matter, and the CNR gain after passive staining. A regression curve was calculated to model CNR gain as a function of the white matter tract thickness (Microsoft Excel 2004). For qualitative analysis, all MRI images acquired after passive staining were reviewed to determine if anatomical structures were resolvable or non resolvable, referring to the mouse lemur brain atlas. We looked for the following nuclei: accumbens (AccN), caudate (CN), septal (SN), hypothalamic (Hyp N), thalamic (Thal), the putamen (Put), globus pallidus (GP), lateral (LGB) and medial (MGB) geniculate bodies; the following white matter tracts: IC, CC, Opt Ch, AC, MTT, Fx and median lemniscus fibers (MLF); the following temporal areas: gyrus dentatus (G Dent), hippocampus (Hipp), subiculum (Sub) and presubiculum (PrSub); and when available, the following olfactory bulb areas: the glomerular layer (GL), the external plexiform layer (ECL), the mitral cell layer (MCL), the internal plexiform layer (IPL), the granule cell layer (GCL), the anterior commissura (AC), the anterior olfactory nucleus (AON) and the olfactory tract (OT). For each structure resolved, its apparent size on MRI images was noted.

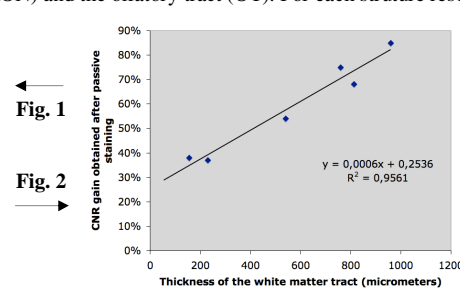


**Table 1**

	Mean apparent thickness
Hippocampus	62 µm
Gyrus dentatus	57 µm
Medial lemniscus fibers	52 µm
Mitral cell layer of the olfactory bulb	31 µm
Internal plexiform layer of the olfactory bulb	31 µm

**RESULTS :** 1) *Quantitative analysis.* Passive staining allowed for a CNR gain of 37 to 85% between grey and white matter. CNR gain was more pronounced around the large white matter tracts; relation between thickness of white matter tracts and CNR gain after passive staining could be modeled by a regression curve (Fig. 2). 2) *Qualitative analysis.* All anatomical structures of interest were resolved on MRI images for each of the 6 brains. The smallest detectable structures are noted in Table 1. The cellular layers of Hipp and G Dent were easily resolvable in each brain and appeared as thin hypointense lines (Fig. 1B). Interestingly, G Dent was always bordered on the outside by a hyperintense rim, which was also found on the acquisition before passive staining; this hyperintense rim was not found on the edge of the Hipp, which may be related to its different cytoarchitecture (Fig. 1B). The cellular layers of the olfactory bulb were also resolved, including the ICL and the MCL which could be differentiated as 2 hyper- and hypointense rims, respectively (Fig. 1E). The different parts of grey matter nuclei were not differentiated, except for the lenticular nucleus, as the GP was significantly more hypointense compared to the Put, due to the higher density of small white matter fibers in GP (Fig. 1C).

LV: lateral ventricle, Vss: vessel

**DISCUSSION :** The passive staining technique allows for a gain of CNR between grey and white matter in formalin-fixed brains. The most probable explanation for this phenomenon is that Gd's hydrophilic properties makes it diffuse easily in the grey matter, which is also hydrophilic, and less easily in the hydrophobic white matter. Given that amyloid deposits are strongly hydrophobic, this passive staining technique should facilitate the ex vivo detection of Aβ deposits in mouse lemurs as previously demonstrated in transgenic mice (3). The regression curve represented in Fig. 2 indicates a theoretical CNR gain of 28% for a 50-micrometer structure, and 31% for a 100-micrometer structure, values which correspond to the common size of amyloid deposits.

**CONCLUSION :** For the first time, we show precise 3D anatomical data on the primate mouse lemur brain by micro-MRI after passive staining, down to the resolution of individual cell layers. The main explanation for the contrast amelioration between grey and white matter after passive staining is a differential diffusion of gadolinium in hydrophobic or hydrophilic environments. Consequently, passive staining should also be useful for increasing the contrast between normal grey matter and amyloid deposits in mouse lemurs, a model of growing interest for AD research.

**ACKNOWLEDGEMENTS :** This work was supported by the France-Alzheimer association and the NIH (R01-AG020197).

**REFERENCES :** (1) Bons N, Rieger F, Prudhomme D, Fisher A, Krause KH. *Microcebus murinus*: a useful primate model for human cerebral aging and Alzheimer's disease? *Genes Brain Behav* 2006;5(2):120-130. (2) Bons N, Silhol S, Barbie V, Mestre-Frances N, Albe-Fessard D. A stereotaxic atlas of the grey lesser mouse lemur brain (*Microcebus murinus*). *Brain Res Bull* 1998;46(1-2):1-173. (3) Dhenain M, Delatour B, Walczak C, Volk A. Passive staining: a novel ex vivo MRI protocol to detect amyloid deposits in mouse models of Alzheimer's disease. *Magn Reson Med* 2006;55(3):687-693.